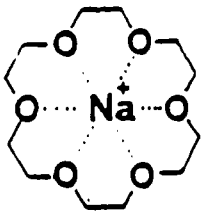

Figure 5. Structure of the cation [Na·18-crown-6]$^+$.

the carbon–carbon bond-forming process was investigated at high carbon dioxide pressure (500 psi) both as a matter of convenience and in order to minimize subsequent carboxylate displacement reactions which are prevalent in the presence of interacting alkali metal ions (eq 3). As can be readily seen in Table VII and

$$M(CO)_5O_2CCH_3^- + Na^+ \xrightarrow{THF} M(CO)_5THF + NaO_2CCH_3 \quad (3)$$

depicted in Figure 4, the cryptand-encapsulated sodium cation exhibits *no* effect on the rate of CO_2 insertion into the W–CH_3^- bond, i.e., the pseudo-first-order rate constant is quite similar to that noted when the non-interacting PPN^+ counterion was employed. This is not totally unexpected since no interaction in solution was observed between the once formed anionic metalloformate or -acetate derivatives and Na(kryptofix-221)$^+$ cation.

On the other hand, there is approximately a 10-fold increase in the rate of CO_2 insertion into $W(CO)_5CH_3^-$ in the presence of $Na(THF)_n^+$ or Na(18-crown-6)$^+$. In the crown ether species (Figure 5), the complex has two open faces which allow access to the anion.[35] Indeed in both the $Na(THF)_n^+$ and Na(18-crown-6)$^+$ derivatives perturbation of the carboxylate ligands by the Na^+ was noted by spectral measurements (Table VI). Concomitantly, more facile loss of the carboxylate ligand was observed during CO_2 insertion reactions involving these counterions. It is worthy of note here that spectroscopic studies have demonstrated that although the rate of cationic exchange in the $NaBPh_4$/18-crown-6/THF system is slow (two ^{23}Na resonances observed in excess Na^+ at −7.9 and −17.1 ppm), the exchange rate is highly dependent on the accompanying anion.[23e]

Acknowledgment. The financial support of this research by the National Science Foundation (Grant CHE 83-08281) is greatly appreciated. We thank J. Nicole White for experimental assistance in some aspects of these investigations.

Registry No. [Na-kryptofix-221][$W(CO)_5O_2CH$], 97860-74-7; [Na-crypt-221][$W(CO)_5CH_3$], 97877-24-2; [PPN][$W(CO)_5CH_3$], 62197-79-9; [PPN][$W(CO)_5O_2CH$], 36499-81-7; CO_2, 124-38-9; ^{13}CO, 1641-69-6.

Supplementary Material Available: A list of observed and calculated structure factors and a table of intermolecular contacts up to 3.8 Å (9 pages). Ordering information is given on any current masthead page.

(35) Interaction of this type have been noted previously, e.g., see ref 10.
(36) In this paper the periodic group notation is in accord with recent actions by IUPAC and ACS nomenclature committees. A and B notation is eliminated because of wide confusion. Groups IA and IIA become groups 1 and 2. The d-transition elements comprise groups 3 through 12, and the p-block elements comprise groups 13 through 18. (Note that the former Roman number designation is preserved in the last digit of the new numbering: e.g., III → 3 and 13.)

Characterization of Five-Coordinate Mono(imidazole)(porphinato)iron(III) Complexes

W. Robert Scheidt,*[1] David K. Geiger,[1] Young Ja Lee,[1] Christopher A. Reed,[2] and G. Lang*[3]

Contribution from the Departments of Chemistry, University of Notre Dame, Notre Dame, Indiana 46556, University of Southern California, Los Angeles, California 90089-1062, and the Department of Physics, Pennsylvania State University, University Park, Pennsylvania 16802.
Received March 4, 1985

Abstract: The preparation of two crystalline forms of [Fe(OEP)(2-MeHIm)]ClO_4 is described. Both crystalline forms have been characterized by X-ray structure determinations, and the five-coordinate group [Fe(OEP)(2-MeHIm)]$^+$ has been confirmed for both. One of the species has also been fully characterized by Mössbauer spectroscopy and temperature-dependent (6-299 K) magnetic susceptibilities. Mössbauer parameters (4.2 K, zero applied field, symmetric doublet) are ΔE_q = 1.39 and δ = 0.40 mm/s for the chloroform solvate. The effective spin is temperature-independent down to ~60 K (μ = 5.9–5.99 μ_B), falling off to 3.7 μ_B at 6 K. The complexes are best described as high-spin species. The temperature dependence of the susceptibility can be fit with a zero-field splitting constant of D = 12 cm^{-1} and weak intermolecular antiferromagnetic coupling ($-J$ = 0.8 cm^{-1}) between adjacent pairs of ions. The Mössbauer data (6-T applied field) are also consistent with these parameters. Crystal data for [Fe(OEP)(2-MeHIm)]ClO_4·$CHCl_3$ are monoclinic, a = 22.786 (6) Å, b = 15.028 (4) Å, c = 49.974 (13) Å, β = 101.70 (2)°, Z = 16, space group $C2/c$, 3933 observed data, and all measurements at 96 K. Crystal data for [Fe(OEP)-(2-MeHIm)]ClO_4·CH_2Br_2 are monoclinic, a = 15.059 (3) Å, b = 19.040 (4) Å, c = 15.093 (3) Å, β = 92.40 (1)°, Z = 4, space group $P2_1/n$, 8658 observed data, R_1 = 0.087, R_2 = 0.092, and all measurements at 100 K. Pertinent structural data are Fe–N_p = 2.038 (6) Å, Fe–N(2-MeHIm) = 2.068 (4) Å; the iron(III) ion is displaced 0.36 Å from the mean porphinato ligand plane (CH_2Br_2 solvate). Pertinent structural data for the chloroform solvate are Fe–N_p = 2.039 (28) Å, Fe–N(2-MeHIm) = 2.09 Å; the iron(III) ion is displaced 0.34 Å from the mean porphinato ligand plane. Both solvates share a common intermolecular π–π interaction between two [Fe(OEP)(2-MeHIm)]$^+$ units. This π–π complex formation is regarded as a significant factor in the isolation of monoligated species rather than the more common bis-ligated ferric complex.

The multiplicity of chemical functions for the hemoproteins continues to arouse curiosity. In attempting to understand how this is achieved in Nature, much attention has been given to the role of the axial ligand(s) in controlling the chemistry and/or the physical properties of the hemoproteins. An imidazole (histidine) residue is a common axial ligand for the heme in hemoproteins. Despite the frequent occurrence of histidine in hemoproteins, the synthetic chemistry of iron porphyrinates having a single imidazole[4]

(1) University of Notre Dame
(2) University of Southern California
(3) Pennsylvania State University

0002-7863/85/1507-5693$01.50/0

ligand is limited. The small number of such iron(II) or iron(III) porphyrinates with a single imidazole ligand is partly the result of thermodynamic constraints; the equilibrium constant (K_2) for the complexing of a second imidazole ligand is more than 1 order of magnitude larger than the constant (K_1) for the binding of the first imidazole ligand[5] to Fe^{II}(Porph) or Fe^{III}(Porph)X. Thus, six-coordinate complexes $[Fe(Porph)(HIm)_2]^{n+}$ (n = 0, 1) have been isolated rather than five-coordinate or mixed-ligand six-coordinate species. The preparation of the five-coordinate species is especially difficult. In the first successful preparation, Collman and Reed used a sterically hindered imidazole ligand, 2-methylimidazole, to obtain high-spin [Fe^{II}(TPP)(2-MeHIm)],[6] a synthetic analogue of deoxymyoglobin. It was expected that the sterically hindered imidazole ligand would reduce the magnitude of K_2 without significantly changing the first (K_1) binding constant owing to the structural differences between the mono-ligated and bis-ligated species. This expectation is realized, although a second 2-methylimidazole binds to ferrous porphyrinates at low temperature.[7] This synthetic strategy has been less successful when applied to ferric porphyrinates; bis(2-methylimidazole) complexes of both Fe^{III}(OEP)[8] and Fe^{III}(TPP)[9] are readily prepared. Ogoshi et al.[10] have reported the synthesis of mono(pyridine) adducts of [$Fe(OEP)OClO_3$]. Whether these species were five- or six-coordinate was not established. Attempts[11] to prepare analogous species using [$Fe(TPP)OClO_3$] yielded only bis adducts even at 1:1 porphyrin ligand ratios; the reasons for Ogoshi et al.'s[10] successful synthesis of mono(pyridine) complexes were unclear to us.[12] Yoshimura et al.[13] have reported the preparation of monoadducts of protohemin chloride with sterically hindered imidazoles; only bis adducts were obtained with sterically unhindered imidazoles. The stereochemical nature of these monoadducts is also not known.

We have investigated the reaction of [$Fe(OEP)OClO_3$] with equimolar amounts of 2-methylimidazole. Under these conditions, we are able to prepare, cleanly, crystalline five-coordinate [Fe(OEP)(2-MeHIm)]$^+$, which has been characterized by Mössbauer spectroscopy, temperature-dependent magnetic susceptibility, and X-ray structure determinations. The X-ray structure determination of two different crystalline forms of [Fe(OEP)(2-MeHIm)]ClO_4 confirms five-coordination in both forms. In addition, the two structure determinations reveal a common intermolecular interaction between two [Fe(OEP)(2-MeHIm)]$^+$ units; this $\pi-\pi$ complex formation may explain the porphinato ligand dependent synthetic differences (e.g., OEP vs. TPP derivatives).

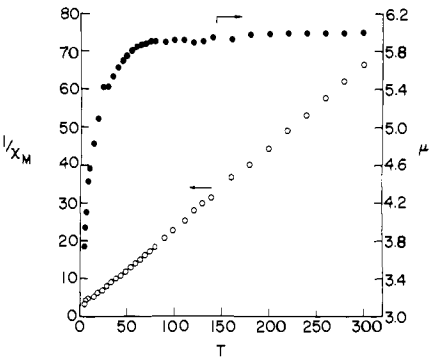

Figure 1. Plot of $1/\chi_M$ vs. T and μ_B vs. T for [Fe(OEP)(2-MeHIm)]ClO_4·$CHCl_3$.

Experimental Section

Synthesis and Physical Data. [$Fe(OEP)OClO_3$] was prepared by the method of Dolphin et al.[14] [Fe(OEP)(2-MeHIm)]ClO_4·$CHCl_3$ was prepared by dissolving 153 mg (0.222 mmol) of [$Fe(OEP)OClO_3$] and 18.2 mg (0.222 mmol) of 2-methylimidazole in 15 mL of chloroform. This solution was divided into nine 5-mL beakers and the vapor from 2:1 hexane/chloroform was allowed to slowly diffuse into the solutions. Single crystals were obtained after 3 days. IR (KBr) ν (ClO_4) 1146, 1090, and 628 cm^{-1}. Isomorphous [Fe(OEP)(1,2-Me_2Im)]ClO_4·$CHCl_3$ was prepared similarly. Because of difficulties in obtaining a completely adequate molecular structure of [Fe(OEP)(2-MeHIm)]ClO_4·$CHCl_3$, as described below, attempts to prepare crystalline samples using other solvents were made. A large variety of halocarbon solvents (required for solubility reasons) were used without success. Finally, satisfactory crystals of [Fe(OEP)(2-MeHIm)]ClO_4·CH_2Br_2 were obtained from methylene bromide solution. These were prepared by dissolving 32.6 mg (0.0473 mmol) of [$Fe(OEP)OClO_3$] in 5 mL of a 9.45 mM solution of 2-methylimidazole in methylene bromide. The solution was gently warmed to facilitate the dissolution of [$Fe(OEP)OClO_3$] and divided into two portions. Each portion was placed over heptane for vapor diffusion. After 5 days, 23.5 mg of single-crystal material was obtained. Additional material could be obtained from the mother liquor by further vapor diffusion with heptane. This crystalline compound suffers from an apparent facile loss of the solvate molecule even on brief exposure to the atmosphere. This difficulty led to use of crystalline [Fe(OEP)(2-MeHIm)]ClO_4·$CHCl_3$ forr all initial physical measurements.

The magnetic susceptibility of [Fe(OEP)(2-MeHIm)]ClO_4·$CHCl_3$ was obtained on ground and unground samples in the solid state over the temperature range 6.0–300 K on a SHE 905 SQUID susceptometer at the University of Southern California. Measurements at 2 kG followed by measurements at 10 kG were identical, indicating an absence of crystal alignment and ferromagnetic impurities. The results are shown in Figure 1. The room temperature moment is 5.99 μ_B. This value is slightly larger than the spin-only moment, the theoretical upper limit. This suggests that the samples had lost a portion of the chloroform solvate and the effective molecular weight should be reduced to reflect the partial occupancy of the solvate in the lattice. A value of 0.76 $CHCl_3$ yields a room-temperature moment of 5.92 μ_B. The Mössbauer spectra of powdered [Fe(OEP)(2-MeHIm)]ClO_4·$CHCl_3$ were obtained on unenriched material using procedures described previously.[15]

X-ray Structure Determination. Preliminary examination of a crystal of [Fe(OEP)(2-MeHIm)]ClO_4·$CHCl_3$ on a Nicolet P$\bar{1}$ diffractometer established a 16-molecule monoclinic unit cell, space group Cc or $C2/c$. Initial data collection was performed at 292 K with use of graphite-monochromated Cu Kα radiation and $\theta - 2\theta$ scans. The space group $C2/c$ was assumed; this requires the presence of two independent molecules of [Fe(OEP)(2-MeHIm)]ClO_4·$CHCl_3$ in the asymmetric unit of structure. The structure was partially solved by using the direct methods program MULTAN78.[16] Most atoms of the two porphinato cores in the

(4) In this paper, imidazole (HIm) is used as a generic term for imidazole itself or any substituted imidazole. Other abbreviations used: Porph, the dianion of a general porphyrin ligand; OEP and TPP, the dianions of octaethylporphyrin and *meso*-tetraphenylporphyrin, respectively; protohemin, the iron(III) derivative of protoporphyrin IX; X, any anionic ligand; 2-MeHIm, 2-methylimidazole; 1-MeIm, 1-methylimidazole; 1,2-Me_2Im, 1,2-dimethylimidazole; N_p, porphinato nitrogen atom; Ct, center of the porphyrin ring, B, neutral nitrogen donor; HRP, horseradish peroxidase.

(5) (a) Yoshimura, T.; Ozaki, T. *Bull. Chem. Soc. Jpn.* **1979**, *52*, 2268-2275. (b) Walker, F. A.; Lo, M.-W.; Ree, M. T. *J. Am. Chem. Soc.* **1976**, *98*, 5552-5560. (c) Coyle, C. L.; Rafson, R. A.; Abbott, E. H. *Inorg. Chem.* **1973**, *12*, 2007-2010.

(6) Collman, J. P.; Reed, C. A. *J. Am. Chem. Soc.* **1973**, *95*, 2048-2049.

(7) Wagner, G. C.; Kassner, R. J. *Biochim. Biophys. Acta* **1975**, *392*, 319-327.

(8) Geiger, D. K.; Lee, Y. J.; Scheidt, W. R. *J. Am. Chem. Soc.* **1984**, *106*, 6339-6343.

(9) Kirner, J. F.; Hoard, J. L.; Reed, C. A. "Abstracts of Papers", 175th National Meeting of the American Chemical Society, Anaheim, CA, March 13-17, 1978; American Chemical Society: Washington, DC, 1978; INOR 14.

(10) Ogoshi, H.; Watanabe, E.; Yoshida, Z. *Chem. Letters* **1973**, 989-992. Ogoshi, H.; Sugimoto, H.; Watanabe, E.; Yoshida, Z.; Maeda, Y.; Sakai, H. *Bull. Chem. Soc. Jpn.* **1981**, *54*, 3414-3419.

(11) Reed, C. A.; Mashiko, T.; Bentley, S. P.; Kastner, M. E.; Scheidt, W. R.; Spartalian, K.; Lang, G. *J. Am. Chem. Soc.* **1979**, *101*, 2948-2958.

(12) Our reinvestigation of Ogoshi's system suggests that it may actually be more complex than reported: Geiger, D. K.; Lee, Y. J.; Scheidt, W. R., work in progress.

(13) Yoshimura, T.; Ozaki, T.; Shintani, Y.; Watanabe, H. *J. Inorg. Nucl. Chem.* **1976**, *38*, 1879-1883. Yoshimura, T.; Ozaki, T.; Shintani, Y. *J. Inorg. Nucl. Chem.* **1977**, *39*, 185-190.

(14) Dolphin, D. H.; Sams, J. R.; Tsin, T. B. *Inorg. Chem.* **1977**, *16*, 711-713.

(15) Mashiko, T.; Kastner, M. E.; Spartalian, K.; Scheidt, W. R.; Reed, C. A. *J. Am. Chem. Soc.* **1978**, *100*, 6354-6362.

(16) Programs used in this study included local modifications of Main, Hull, Lessinger, Germain, Declerq, and Woolfson's MULTAN78, Jacobson's ALFF and ALLS, Busing and Levy's ORFFE and ORFLS, and Johnson' ORTEP2. Atomic form factors were from: Cromer, D. T.; Mann, J. B. *Acta Crystallogr., Sect. A* **1968**, *A24*, 321-323. Real and imaginary corrections for anomalous dispersion in the form factor of the iron, chlorine, and bromine atoms were from: Cromer, D. T.; Liberman, D. J. *J. Chem. Phys.* **1970**, *53*, 1891-1898. Scattering factors for hydrogen were from: Stewart, R. F.; Davidson, E. R.; Simpson, W. T. *Ibid.* **1965**, *42*, 3175-3187.

Table I. Summary of Crystal Data and Intensity Collection Parameters

compd	[Fe(OEP)-(2-MeHIm)]-$ClO_4 \cdot CHCl_3$	[Fe(OEP)-(2-MeHIm)]-$ClO_4 \cdot CH_2Br_2$
formula	$FeCl_4O_4N_6C_{41}H_{51}$	$FeBr_2ClO_4N_6C_{41}H_{52}$
fw, amu	889.56	944.01
temp, K	96 ± 5	100 ± 5
a, Å	22.786 (6)	15.059 (3)
b, Å	15.028 (4)	19.040 (4)
c, Å	49.974 (13)	15.093 (3)
β, deg	101.70 (2)	92.40 (1)
V, Å^3	16757	4324
Z	16	4
space group	C2/c	$P2_1/n$
d_{calcd}, g/cm^3	1.41	1.450
d_{meas}, g/cm^3	1.32[a]	1.41[a]
radiat	graphite-monochromated Cu Kα (λ = 1.5418)	graphite-monochromated Mo Kα = (λ = 0.71073)
scan techniq	$\theta - 2\theta$	$\theta - 2\theta$
background	0.5 times scan at extreme of scan	profile analysis
scan rate, deg/min	3–24	2–12
scan range, deg	0.65 below Kα_1 0.65 above Kα_2	0.70 below Kα_1 0.70 above Kα_2
μ, mm^{-1}	5.69	2.28
2θ limits, deg	3.5–94.9	3.5–62.10
cryst dimens, mm	1.17 × 0.53 × 0.17	0.4 × 0.5 × 0.8
criter for observn	$F_0 > 3\sigma(F_0)$	$F_0 > 3\sigma(F_o)$
unique obsd data	3933	8658
data/param	7.6	16.6
R_1	0.175	0.087
R_2	0.174	0.092
goodness of fit	3.87	2.54

[a] Measured at 292 K.

asymmetric unit of structure were located. However, some of the remaining atoms were never satisfactorily located; the difficulties appeared to result, in part, from large thermal motion. Accordingly, intensity data were remeasured at 96 K with use of an LT-1 low-temperature attachment for the diffractometer. Intensity data collection parameters and final refined cell constants are listed in Table I. Net intensities were reduced as described previously.[17] An empirical absorption correction was applied to the data.[18] A complete structure solution was obtained from this low-temperature data set, although a number of difficulties were encountered. The final structure was considered only partially satisfactory; complete details are reported as supplementary material. Tables IS and IIS report final atomic coordinates and isotropic temperature factors, Table IIIS reports the anisotropic temperature factors for the 17 atoms refined anisotropically, Tables IVS and VS give the individual bond distances and angles, respectively. Table VIS is a listing of the observed and calculated structure amplitudes (×10). Figures 1S and 2S are ORTEP plots of the two independent [Fe(OEP)(2-MeHIm)]$^+$ ions; Figures 3S and 4S illustrate some features of the interactions between adjacent [Fe(OEP)(2-MeHIm)]$^+$ ions.

Preliminary examination of crystals of [Fe(OEP)(2-MeHIm)]-$ClO_4 \cdot CH_2Br_2$ established a four-molecule monoclinic unit cell, with the uniquely defined space group $P2_1/n$. These preliminary measurements also revealed a serious decrease in the X-ray intensity on exposure to the atmosphere. All subsequent measurements were made at 100 K; this eliminated the problem of the secular decrease in the intensities of the diffraction maxima. The final values of cell constants and the intensity data collection parameters are listed in Table I. An extensive data set was collected at the lower temperature; data were corrected for absorption by using a semiempirical technique.[18] Four standard reflections, measured every 50 reflections during data collection, showed no trends. A total of 8658 reflections having $(\sin\theta)/\lambda < 0.726$ Å^{-1} and $F_o > 3\sigma(F_o)$ was retained as observed (63% of the theoretical number possible) and was used in the solution and refinement of structure.

(17) Scheidt, W. R. *J. Am. Chem. Soc.* **1974**, *96*, 84-89.
(18) North, A. C. T.; Phillips, D. C.; Matthews, F. S. *Acta Crystallogr., Sect. A* **1968**, *24*, 351-359.

Table II. Fractional Coordinates[a]

atom	X	Y	Z
Fe	0.511 41 (4)	0.893 10 (4)	0.042 79 (4)
Br(1)	0.214 15 (5)	0.082 86 (4)	0.384 48 (4)
Br(2)	0.241 91 (7)	−0.070 10 (5)	0.465 40 (5)
Cl	0.558 90 (7)	0.511 30 (6)	0.196 92 (8)
N(1)	0.642 02 (23)	0.909 89 (20)	0.020 01 (24)
N(2)	0.540 93 (24)	0.907 26 (20)	0.174 07 (24)
N(3)	0.380 82 (22)	0.910 71 (19)	0.067 57 (23)
N(4)	0.482 57 (22)	0.917 60 (20)	−0.086 87 (23)
N(5)	0.507 26 (22)	0.785 27 (21)	0.026 84 (23)
N(6)	0.515 84 (27)	0.671 71 (22)	0.040 92 (27)
C(a1)	0.680 27 (27)	0.912 52 (23)	−0.061 79 (29)
C(a2)	0.712 85 (27)	0.908 38 (25)	0.081 94 (29)
C(a3)	0.624 6 (3)	0.907 62 (24)	0.215 80 (29)
C(a4)	0.481 6 (3)	0.908 20 (23)	0.241 67 (28)
C(a5)	0.343 00 (29)	0.908 69 (23)	0.148 93 (29)
C(a6)	0.310 99 (28)	0.914 25 (24)	0.005 28 (29)
C(a7)	0.399 43 (28)	0.918 92 (24)	−0.128 38 (28)
C(a8)	0.541 07 (27)	0.917 75 (23)	−0.154 28 (26)
C(b1)	0.776 13 (27)	0.911 66 (23)	−0.051 2 (3)
C(b2)	0.796 05 (29)	0.908 52 (24)	0.038 5 (3)
C(b3)	0.617 3 (3)	0.906 97 (24)	0.310 7 (3)
C(b4)	0.529 4 (4)	0.907 49 (24)	0.327 02 (29)
C(b5)	0.247 40 (29)	0.909 26 (22)	0.137 7 (3)
C(b6)	0.227 18 (26)	0.913 22 (23)	0.048 64 (29)
C(b7)	0.405 91 (27)	0.918 78 (23)	−0.223 85 (27)
C(b8)	0.494 41 (28)	0.917 55 (23)	−0.239 60 (27)
C(m1)	0.633 29 (27)	0.915 98 (24)	−0.142 13 (29)
C(m2)	0.703 58 (29)	0.907 31 (25)	0.172 8 (3)
C(m3)	0.390 5 (3)	0.907 94 (23)	0.229 41 (29)
C(m4)	0.319 47 (27)	0.918 15 (24)	−0.085 24 (29)
C(11)	0.838 60 (29)	0.911 81 (26)	−0.126 2 (3)
C(12)	0.855 3 (4)	0.839 2 (3)	−0.162 6 (4)
C(21)	0.886 5 (3)	0.905 63 (27)	0.084 1 (3)
C(22)	0.911 4 (3)	0.833 3 (3)	0.119 3 (4)
C(31)	0.695 3 (4)	0.902 95 (27)	0.376 3 (3)
C(32)	0.730 8 (4)	0.829 4 (3)	0.387 4 (4)
C(41)	0.485 9 (4)	0.906 76 (26)	0.414 7 (3)
C(42)	0.450 2 (4)	0.834 86 (28)	0.439 0 (3)
C(51)	0.184 4 (3)	0.904 66 (27)	0.212 1 (3)
C(52)	0.174 3 (4)	0.830 3 (3)	0.246 3 (4)
C(61)	0.137 48 (29)	0.914 26 (27)	0.001 2 (3)
C(62)	0.108 6 (3)	0.842 85 (29)	−0.033 2 (4)
C(71)	0.328 3 (3)	0.916 41 (25)	−0.289 71 (29)
C(72)	0.292 6 (3)	0.842 7 (3)	−0.304 5 (4)
C(81)	0.537 89 (29)	0.913 29 (24)	−0.327 02 (28)
C(82)	0.569 7 (3)	0.838 92 (27)	−0.347 5 (3)
C(1)	0.525 86 (29)	0.733 32 (27)	0.082 5 (3)
C(2)	0.485 5 (3)	0.754 1 (3)	−0.054 7 (3)
C(3)	0.491 2 (4)	0.683 38 (29)	−0.046 2 (3)
C(4)	0.552 7 (4)	0.737 9 (3)	0.178 7 (3)
C(5)	0.161 3 (3)	0.006 9 (4)	0.444 5 (4)
O(1)	0.481 7 (7)	0.487 3 (7)	0.229 8 (9)
O(2)	0.596 1 (9)	0.564 7 (6)	0.242 6 (8)
O(3)	0.619 1 (6)	0.456 1 (6)	0.182 2 (7)
O(4)	0.551 5 (5)	0.536 59 (24)	0.108 0 (3)
O(5)	0.478 3 (8)	0.534 8 (9)	0.226 8 (9)
O(6)	0.626 9 (7)	0.535 9 (7)	0.266 6 (8)
O(7)	0.559 9 (10)	0.436 8 (5)	0.202 5 (7)

[a] The estimated standard deviations of the least significant digits are given in parentheses.

The structure was solved by direct methods[16] and standard difference Fourier techniques. The perchlorate anion was found to be disordered; the model had two perchlorate positions rotated by 35° around the Cl–O(4) vector and a common Cl center. The two sets of the three remaining perchlorate oxygen atoms were assigned occupancy factors of 0.5 for each atom. After preliminary full-matrix least-squares refinement, difference Fourier maps revealed the position of all meso hydrogen atoms, all imidazole hydrogen atoms, and most of the ethyl group hydrogen atoms. All hydrogen atoms were included in the subsequent cycles of least-squares refinement as fixed contributors (C–H = 0.95 Å, N–H = 0.87 Å, and B(H) = B(C or N) + 1.0 Å^2). Least-squares refinement was then carried to convergence for the 522 parameters which included anisotropic temperature factors for all heavy atoms. The parameters were refined in two large groups with all iron and bromine parameters included in both blocks. At convergence, $R_1 = 0.087$ and $R_2 = 0.092$,[19] with a final data/parameter ratio of 16.6. A final difference

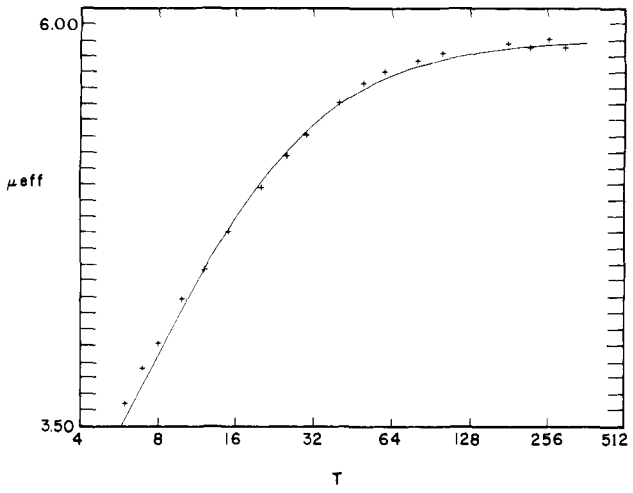

Figure 2. Comparison of observed and calculated values of μ_B vs. T for [Fe(OEP)(2-MeHIm)]ClO_4·$CHCl_3$. Calculated values are based on D = 12 cm^{-1} and $-J$ = 0.8 cm^{-1}. In this figure, the measured moments have been multiplied by 0.984 to reflect possible partial loss of the solvate molecule (cf. Experimental Section).

Fourier map had the six highest peaks (0.81–1.19 e/Å) associated with the bromine atoms and the perchlorate anion; the map was judged to be otherwise featureless. Final values of the atomic coordinates are reported in Table II. The final anisotropic temperature factors and the fixed hydrogen atom positions are reported in Tables VIIS and VIIIS, respectively, of the supplementary material. The final observed and calculated structure amplitudes (×10) are given in Table IXS.

Results and Discussion

The synthesis of five-coordinate [Fe(OEP)(2-MeHIm)]ClO_4 can be accomplished by the reaction of 1:1 2-MeHIm:[Fe(OEP)$OClO_3$]. Careful control of stoichiometry (and perhaps the other conditions specified in the experimental) is important; only the bis complex is isolated[8] at ligand-to-porphyrin ratios as small as 5. All crystalline samples of [Fe(OEP)(2-MeHIm)]ClO_4 appear to be homogeneous by spectroscopic critera and single-crystal X-ray examination. Physical measurements were made on the chloroform solvate of [Fe(OEP)(2-MeHIm)]ClO_4 as this species retained its crystallinity under ambient conditions.

Mössbauer data were obtained both in the presence and absence of an applied external field. In zero field, an symmetric quadrupole doublet was observed with ΔE_q and δ of 1.39 and 0.40 mm/s at 4.2 K. (Values are relative to Fe metal.) The isomer shift is that expected for ferric complexes; the quadrupole splitting constant is larger than that normally observed[20] for high-spin five-coordinate [Fe(P)X] complexes (X = anion). The observed quadrupole splitting is in the middle of values previously reported[15,21,22] for high-spin six-coordinate porphyrinate systems. Mössbauer spectra at high field (6 T, 4.2–128 K) and at intermediate fields (1–4 T, 4.2 K) were measured for fits of the antiferromagnetic coupling constant J and the zero-field splitting constant D.

The magnetic susceptibility as a function of temperature is shown in Figure 1. The room-temperature moment and the general form of the temperature-dependent magnetic susceptibility is that expected for a high-spin iron(III) porphyrinate with a large zero-field splitting.[23] However, the susceptibility data cannot be fit with only zero-field splitting. A satisfactory fit of the data can be made by using a zero-field constant of 12 cm^{-1} and weak

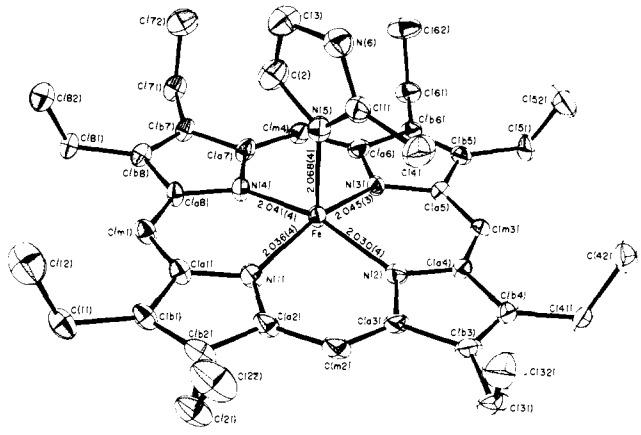

Figure 3. Computer drawn model, in perspective, of [Fe(OEP)(2-MeHIm)]ClO_4·CH_2Br_2. The labels for all atoms of the molecule are displayed: 50% probability ellipsoids are drawn for all atoms.

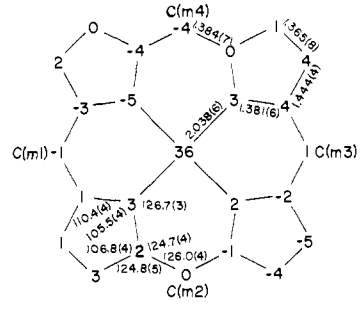

Figure 4. Formal diagram of a porphinato core displaying the average values for the bond parameters. Also displayed are the perpendicular displacements, in units of 0.01 Å, of each atom from the mean plane of the core.

antiferromagnetic coupling ($-J$ = 0.8 cm^{-1}) between pairs of [Fe(OEP)(2-MeHIm)]$^+$. This weak antiferromagnetic coupling is consistent with the solid-state structure (vide infra). Since the interaction between pairs of [Fe(OEP)(2-MeHIm)]$^+$ ions differs only in detail between the two crystalline forms, it can be expected that the temperature-dependent magnetic susceptibilities will be similar for the methylene bromide solvate. Measurement of susceptibilities and Mössbauer spectra of this difficult-to-handle crystalline form are being attempted; complete details will be published elsewhere. Preliminary Mössbauer data for the methylene bromide solvate are similar to those observed for the chloroform solvate.[24] We conclude that [Fe(OEP)(2-MeHIm)]ClO_4 has a high-spin state that is modulated by a weak antiferromagnetic interaction from an adjacent molecule. The magnitude of the antiferromagnetic interaction suggests that it must result from coupling through the porphyrin π system; dipolar coupling would lead to a much smaller value of J. Figure 2 shows the agreement between the observed temperature-dependent susceptibility data and that calculated by using the above values of D and J.

The structure of the [Fe(OEP)(2-MeHIm)]$^+$ ion has been determined with use of two different crystalline forms of the complex. The first, [Fe(OEP)(2-MeHIm)]ClO_4·$CHCl_3$, crystallizes with two independent molecules in the asymmetric unit of structure. Although the analysis of structure of this solvate is not wholly adequate, the structure of the two independent ions is identical within experimental error. Moreover, all essential structural features are in agreement with those found for the second form, [Fe(OEP)(2-MeHIm)]ClO_4·CH_2Br_2. All details of the structure determination of the chloroform solvate are given in the supplementary material. Complete details for [Fe(OEP)(2-MeHIm)]ClO_4·CH_2Br_2 are given herein.

(19) $R_1 = \sum||F_o| - |F_c||/\sum|F_o|$ and $R_2 = [\sum w(|F_o| - |F_c|)^2/\sum w(F_o)^2]^{1/2}$

(20) Sams, J. R.; Tsin, T. B. In "The Porphyrins"; Dolphin, D., Ed.; Academic Press: New York, 1979; Vol. IV, p 441.

(21) Scheidt, W. R.; Cohen, I. A.; Kastner, M. E. *Biochemistry* **1979**, *18*, 3546-3552.

(22) Gans, P.; Buisson, G.; Duee, E.; Regnard, J.-R.; Marchon, J.-C. *J. Chem. Soc., Chem. Commun.* **1979**, 393-394.

(23) Mitra, S. In "Physical Bioinorganic Chemistry—Iron Porphyrins, Part II"; Lever, A. B. P., Gray, H. B., Eds.; Addison-Wesley: Reading, MA, 1983; pp 1-42.

(24) Values for the quadrupole splitting and isomer shift are 1.40 and 0.40 mm/s. The preliminary value for $-J$ is 0.5.

Table III. Bond Lengths in $[Fe(OEP)(2\text{-MeHIm})]ClO_4 \cdot CH_2Br_2$[a]

type	dist, Å	type	dist, Å
Fe–N(I)	2.036 (4)	C(b7)–C(b8)	1.364 (6)
Fe–N(2)	2.030 (4)	C(b1)–C(11)	1.502 (6)
Fe–N(3)	2.045 (3)	C(b2)–C(21)	1.501 (6)
Fe–N(4)	2.041 (4)	C(b3)–C(31)	1.506 (7)
Fe–N(5)	2.068 (4)	C(b4)–C(41)	1.501 (6)
N(1)–C(a1)	1.385 (5)	C(b5)–C(51)	1.503 (6)
N(1)–C(a2)	1.389 (5)	C(b6)–C(61)	1.502 (6)
N(2)–C(a3)	1.385 (6)	C(b7)–C(71)	1.503 (6)
N(2)–C(a4)	1.384 (6)	C(b8)–C(81)	1.500 (6)
N(3)–C(a5)	1.376 (5)	C(11)–C(12)	1.513 (7)
N(3)–C(a6)	1.382 (6)	C(21)–C(22)	1.518 (7)
N(4)–C(a7)	1.376 (5)	C(31)–C(32)	1.505 (8)
N(4)–C(a8)	1.373 (5)	C(41)–C(42)	1.522 (7)
C(a1)–C(m1)	1.380 (6)	C(51)–C(52)	1.517 (7)
C(a2)–C(m2)	1.385 (6)	C(61)–C(62)	1.513 (7)
C(a3)–C(m2)	1.378 (6)	C(71)–C(72)	1.517 (7)
C(a4)–C(m3)	1.377 (7)	C(81)–C(82)	1.530 (7)
C(a5)–C(m3)	1.383 (6)	N(5)–C(1)	1.320 (6)
C(a6)–C(m4)	1.379 (6)	N(5)–C(2)	1.393 (6)
C(a7)–C(m4)	1.393 (6)	N(6)–C(1)	1.336 (6)
C(a8)–C(m1)	1.394 (6)	N(6)–C(3)	1.369 (6)
C(a1)–C(b1)	1.446 (6)	C(1)–C(4)	1.494 (7)
C(a2)–C(b2)	1.438 (6)	C(2)–C(3)	1.355 (8)
C(a3)–C(b3)	1.441 (6)	Cl–O(1)	1.362 (10)
C(a4)–C(b4)	1.449 (6)	Cl–O(2)	1.338 (11)
C(a5)–C(b5)	1.442 (6)	Cl–O(3)	1.411 (8)
C(a6)–C(b6)	1.446 (6)	Cl–O(4)	1.426 (5)
C(a7)–C(b7)	1.448 (6)	Cl–O(5)	1.386 (11)
C(a8)–C(b8)	1.441 (6)	Cl–O(6)	1.511 (10)
C(b1)–C(b2)	1.375 (6)	Cl–O(7)	1.421 (10)
C(b3)–C(b4)	1.355 (7)	C(5)–Br(1)	1.898 (6)
C(b5)–C(b6)	1.367 (6)	C(5)–Br(2)	1.921 (6)

[a] The numbers in parentheses are the estimated standard deviations.

The structure of the $[Fe(OEP)(2\text{-MeHIm})]^+$ ion, determined at 100 K, is shown in Figure 3. The figure illustrates the labeling scheme for all atoms used in the tables. Listings of individual bond distances and bond angles are given in Tables III and IV, respectively. Averaged values for the unique chemical classes of distances and angles in the prophinato core are entered on the formal diagram given in Figure 4. Also shown in Figure 4 are the perpendicular displacements of each atom, in units of 0.01 Å, from the mean plane of the 24-atom core. The deviations from exact planarity are not noteworthy.

The imidazole ligand, including the substituent methyl group, is planar to within ±0.006 Å. The dihedral angle between the imidazole plane and the porphinato core is 88.1°. The Fe–N(5) vector is tipped by 5° from the heme normal, leading to unequal N_p–Fe–N(5) angles; the effect of this tipping is to increase the separation between the imidazole methyl group and atoms of the porphinato core (cf. Figure 2). The nonequal Fe–N(5)–C(1) (137.7 (3)°) and Fe–N(5)–C(2) (121.1 (3)°) angles is also an important contributor to increasing the C(4)···core atom separation. The N(6) proton of the 2-methylimidazole is hydrogen bonded to the O(4) perchlorate oxygen with the N(6)···O(4) separation = 2.808 Å. The imidazole plane is almost directly over the N(4)FeN(2) coordinate plane; the projection of the imidazole onto the porphinato core makes a 3.9° angle with the Fe–N(4) bond.[25] The orientation of the imidazole methyl group hydrogen atoms was determined; all three hydrogen atoms were located in difference Fourier syntheses. All angles subtended at C(4) are within 2° of their ideal tetrahedral values. One hydrogen atom is directed away from the porphinato core; this C(4)–H vector is within 1° of coplanarity with the imidazole plane. This orientation is the most satisfactory one to minimize nonbonded contacts between the methyl hydrogen atoms and porphinato core atoms.

The axial Fe–N(HIm) bond distance is 2.068 (4) Å for the methylene bromide solvate; the corresponding distances for the chloroform solvate are 2.09 and 2.10 Å. This distance and other parameters for a number of five-coordinate imidazole-ligated metalloporphyrins are compared[26–31] in Table V. As can be seen from the table, the axial bond length in the [Fe(OEP)(2-Me-

Table IV. Bond Angles in $[Fe(OEP)(2\text{-MeHIm})]ClO_4 \cdot CH_2Br_2$[a]

angle	degrees	angle	degrees
N(1)FeN(2)	88.3 (1)	C(a3)C(b3)C(31)	124.2 (5)
N(1)FeN(3)	161.5 (2)	C(b4)C(b3)C(31)	128.4 (4)
N(1)FeN(4)	88.3 (1)	C(a4)C(b4)C(b3)	106.9 (4)
N(1)FeN(5)	98.3 (1)	C(a4)C(b4)C(41)	124.4 (5)
N(2)FeN(3)	88.4 (1)	C(b3)C(b4)C(41)	128.7 (4)
N(2)FeN(4)	159.2 (2)	C(a5)C(b5)C(b6)	107.2 (4)
N(2)FeN(5)	104.5 (1)	C(a5)C(b5)C(51)	124.7 (4)
N(3)FeN(4)	88.3 (1)	C(b6)C(b5)C(51)	128.0 (4)
N(3)FeN(5)	99.2 (1)	C(a6)C(b6)C(b5)	106.4 (4)
N(4)FeN(5)	96.4 (1)	C(a6)C(b6)C(61)	124.7 (4)
FeN(1)C(a1)	126.6 (3)	C(b5)C(b6)C(61)	128.9 (4)
FeN(1)C(a2)	127.1 (3)	C(a7)C(b7)C(b8)	106.3 (4)
C(a1)N(1)C(a2)	105. (3)	C(a7)C(b7)C(71)	125.1 (4)
FeN(2)C(a3)	127.0 (3)	C(b8)C(b7)C(71)	128.5 (4)
FeN(2)C(a4)	126.8 (3)	C(a8)C(b8)C(b7)	106.7 (4)
C(a3)N(2)C(a4)	105.5 (4)	C(a8)C(b8)C(81)	124.9 (4)
FeN(3)C(a5)	126.6 (3)	C(b7)C(b8)C(81)	128.3 (4)
FeN(3)C(a6)	126.4 (3)	C(a1)C(m1)C(a8)	126.0 (4)
C(a5)N(3)C(a6)	106.1 (3)	C(a2)C(m2)C(a3)	126.2 (4)
FeN(4)C(a7)	126.4 (3)	C(a4)C(m3)C(a5)	126.4 (4)
FeN(4)C(a8)	126.4 (3)	C(a6)C(m4)C(a7)	125.5 (4)
C(a7)N(4)C(a8)	105.2 (3)	C(b1)C(11)C(12)	113.0 (4)
FeN(5)C(1)	131.7 (3)	C(b2)C(21)C(22)	113.5 (4)
FeN(5)C(2)	122.1 (3)	C(b3)C(31)C(32)	112.6 (4)
C(1)N(5)C(2)	106.1 (4)	C(b4)C(41)C(42)	113.1 (4)
C(1)N(6)C(3)	109.2 (4)	C(b5)C(51)C(52)	112.6 (4)
N(1)C(a1)C(b1)	110.6 (4)	C(b6)C(61)C(62)	113.0 (4)
N(1)C(a1)C(m1)	124.6 (4)	C(b7)C(71)C(72)	112.7 (4)
C(b1)C(a1)C(m1)	124.8 (4)	C(b8)C(81)C(82)	112.3 (4)
N(1)C(a2)C(b2)	110.6 (4)	N(5)C(1)N(6)	110.0 (4)
N(1)C(a2)C(m2)	124.1 (4)	N(5)C(1)C(4)	128.1 (5)
C(b2)C(a2)C(m2)	125.3 (4)	N(6)C(1)C(4)	121.9 (4)
N(2)C(a3)C(b3)	110.2 (4)	N(5)C(2)C(3)	109.2 (4)
N(2)C(a3)C(m2)	124.9 (4)	N(6)C(3)C(2)	105.4 (4)
C(b3)C(a3)C(m2)	124.8 (4)	O(1)ClO(2)	114.3 (9)
N(2)C(a4)C(b4)	110.0 (4)	O(1)ClO(3)	111.8 (8)
N(2)C(a4)C(m3)	124.8 (4)	O(1)ClO(4)	115.0 (6)
C(b4)C(a4)C(m3)	125.1 (4)	O(1)ClO(5)	38.5 (7)
N(3)C(a5)C(b5)	110.1 (4)	O(1)ClO(6)	114.5 (8)
N(3)C(a5)C(m3)	124.5 (4)	O(1)ClO(7)	69.5 (8)
C(b5)C(a5)C(m3)	125.4 (4)	O(2)ClO(3)	112.9 (7)
N(3)C(a6)C(b6)	110.2 (4)	O(2)ClO(4)	104.0 (6)
N(3)C(a6)C(m4)	125.2 (4)	O(2)ClO(5)	86.6 (9)
C(b6)C(a6)C(m4)	124.6 (4)	O(2)ClO(6)	31.7 (6)
N(4)C(a7)C(b7)	110.8 (4)	O(2)ClO(7)	136.4 (7)
N(4)C(a7)C(m4)	125.1 (4)	O(3)ClO(4)	97.4 (5)
C(b7)C(a7)C(m4)	124.1 (4)	O(3)ClO(5)	150.2 (9)
N(4)C(a8)C(b8)	111.0 (3)	O(3)ClO(6)	85.4 (7)
N(4)C(a8)C(m1)	124.7 (4)	O(3)ClO(7)	42.3 (6)
C(b8)C(a8)C(m1)	124.3 (4)	O(4)ClO(5)	99.3 (6)
C(a1)C(b1)C(b2)	106.6 (4)	O(4)ClO(6)	125.0 (5)
C(a1)C(b1)C(11)	124.8 (4)	O(4)ClO(7)	113.2 (5)
C(b2)C(b1)C(11)	128.6 (4)	O(5)ClO(6)	104.5 (8)
C(a2)C(b2)C(b1)	106.9 (4)	O(5)ClO(7)	108.0 (9)
C(a2)C(b2)C(21)	125.6 (4)	O(6)ClO(7)	105.2 (7)
C(b1)C(b2)C(21)	127.5 (4)	Br(1)C(5)Br(2)	112.7 (3)
C(a3)C(b3)C(b4)	107.3 (4)		

[a] The numbers in parentheses are the estimated standard deviations.

(25) The angle between the ligand plane projection and the closest M–N_p vector is denoted ϕ throughout this paper.

(26) Kirner, J. F.; Reed, C. A.; Scheidt, W. R. *J. Am. Chem. Soc.* **1977**, *99*, 2557-2563.
(27) Collman, J. P.; Kim, N.; Hoard, J. L.; Lang, G.; Radanovich, L. J.; Reed, C. A. "Abstracts of Papers", 167th National Meeting of the American Chemical Society, Los Angeles, CA, April 1974; American Chemical Society; Washington, DC, 1974; INOR 29.
(28) Jameson, G. B.; Molinaro, F. S.; Ibers, J. A.; Collman, J. P.; Brauman, J. I.; Rose, E.; Suslick, K. S. *J. Am. Chem. Soc.* **1980**, *102*, 3224-3237.
(29) Scheidt, W. R. *J. Am. Chem. Soc.* **1974**, *96*, 90-94.
(30) Dwyer, P. N.; Madura, P.; Scheidt, W. R. *J. Am. Chem. Soc.* **1974**, *96*, 4815-4819.
(31) Little, R. G.; Ibers, J. A. *J. Am. Chem. Soc.* **1974**, *96*, 4452-4463.

Table V. Comparison of Five-Coordinate Imidazole-Ligated Metalloporphyrins

complex	M–N_p[a]	M–N(HIm)[a]	Δ[a,b]	ϕ[c]	ref
[Mn(TPP)(1-MeIm)]	2.128 (7)	2.192 (2)	0.56	15.4	26
[Fe(OEP)(2-MeHIm)]$^+$ CH_2Br_2 solvate	2.038 (6)	2.068 (4)	0.36	4.0	this work
[Fe(OEP)(2-MeHIm)]$^+$ $CHCl_3$ solvate	2.039 (28)	2.09	0.34	7.3	this work
		2.10	0.33	3.0	
[Fe(TPP)(2-MeHIm)]	2.086 (4)	2.161 (5)	0.42	7.4	27
[Fe(TpivPP)(2-MeHIm)]	2.072 (5)	2.095 (6)	0.40	22.8	28
[Co(TPP)(1-MeIm)]	1.977 (6)	2.157 (3)	0.14	0	29
[Co(TPP)(1,2-Me_2Im)]	1.985 (3)	2.216 (2)	0.18	20	30
[Co(OEP)(1-MeIm)]	1.96 (1)	2.15 (1)	0.16	10	31

[a] Values in angstroms. [b] Δ is displacement of the metal atom from the 24-atom mean plane in angstroms. [c] Values in degrees.

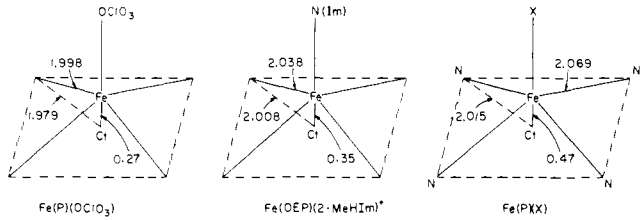

Figure 5. Schematic representations of the idealized (C_{4v} symmetry) coordination groups of intermediate-spin [Fe(Porph)$OClO_3$] and [Fe(OEP)(2-MeHIm)]$^+$ and high-spin [Fe(Porph)X].

HIm)]$^+$ complexes is significantly shorter than any of the observed M–N(HIm) distances in the high-spin d^5 or d^6 and low-spin d^7 species listed in Table V. Some years ago, Hoard suggested[32] that the axial bond distance in high-spin five-coordinate iron(III) porphyrinates would be as short as that bond in an analogous low-spin ferric complex. This has, in fact, been found for a number of such species where the axial ligand is an anion, viz., Fe(TPP)(NCS)[33] and Fe(TPP)(NCS)(py).[34] However, this pattern is not quite followed in [Fe(OEP)(2-MeHIm)]$^+$; the axial bond distance is still longer than the distance in the low-spin complex [Fe(TPP)(2-MeHIm)$_2$]ClO_4[9] (axial distances 2.015 and 2.010 Å) but is significantly shorter than the high-spin distance[8] (2.275 (1) Å in [Fe(OEP)(2-MeHIm)$_2$]ClO_4). It is possible that the combination of unfavorable orientation (small ϕ angle) and steric bulk of the axial ligand serve to increase the axial Fe–N(N(HIm) bond length.

The average equatorial Fe–N_p bond distance is 2.038 (6) Å. The iron(III) ion is displaced 0.36 Å from the mean plane of the 24-atom core and 0.35 Å from the mean plane of the four nitrogen atoms. These coordination group parameters are significantly smaller than those observed for the class of high-spin complexes, [Fe(Porph)X], which have values tightly clustered around the average.[35] A comparison of values for [Fe(OEP)(2-MeHIm)]$^+$, [Fe(Porph)X], and the five-coordinate admixed intermediate-spin complexes [Fe(Porph)$OClO_3$][11,36] is given in Figure 5. The decrease in the values of the interrelated Fe–N_p and Δ distances for [Fe(OEP)(2-MeHIm)]$^+$ relative to the [Fe(Porph)X] derivatives must result from the overall positive charge. Without the charge compensation from an anionic axial ligand, there is an increased charge attraction of the Fe(III) ion for the negatively charged porphinato ligand. The nearly identical values found for the chloroform solvate (Table V) lead us to suggest that decreased Fe–N_p bond distances will be a real feature of all high-spin [Fe(Porph)(B)]$^+$ species. It should be noted that the 2.038 (6) ÅFe–N_+ distance in [Fe(OEP)(2-MeHIm)]$^+$ is even smaller[37]

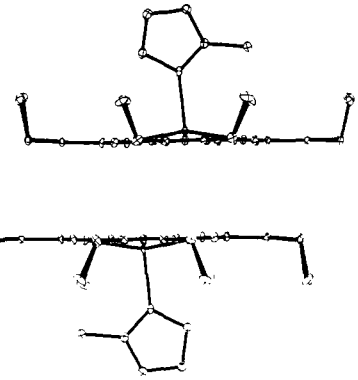

Figure 6. Computer-drawn model of the two [Fe(OEP)(2-MeHIm)]$^+$ ions related by an inversion center which shows the overlap of the two cores. The two porphinato cores are perpendicular to the plane of the drawing: 15% probability ellipsoids are given.

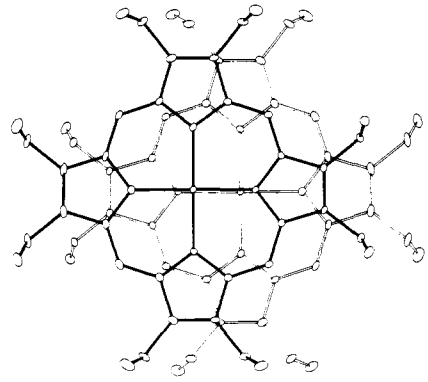

Figure 7. Second view of the π–π dimer. The planes of the two parallel porphinato cores are also parallel to the plane of the paper, and the heavy-lined core is closest to the viewer. For clarity, the 2-MeHIm ligands have been omitted.

than the average 2.045-Å value found for cationic high-spin *six*-coordinate [Fe(TPP)L_2]$^+$ complexes.[15,21]

The ferric hemoproteins with a coordination group most similar to that of [Fe(OEP)(2-MeHIm)]$^+$ are cytochrome *c′* and horseradish peroxidase (HRP). Five-coordination in cytochrome *c′* from *Rhodospirillum molischianum* has been confirmed by a crystal structure analysis.[38] Evidence for five-coordination in HRP comes from photolysis,[39] resonance Raman,[40] and NMR experiments,[41] although some uncertainity as to the coordination number

(32) Hoard, J. L. In "Structural Chemistry and Molecular Biology"; Rich, A., Davidson, N., Eds.; W. H. Freeman: San Francisco, CA; 1968; pp 573-594.

(33) Bloom, A.; Hoard, J. L. "Abstracts of Papers", 173rd National Meeting of the American Chemical Society, New Orleans, New Orleans, LA, March 21-25, 1977; American Chemical Society: Washington, DC, 1977; INOR 27.

(34) Scheidt, W. R.; Lee, Y. J.; Geiger, D. K.; Taylor, K.; Hatano, K. *J. Am. Chem. Soc.* **1982**, *104*, 3367-3374.

(35) Scheidt, W. R.; Reed, C. A. *Chem. Rev.* **1981**, *81*, 543-555.

(36) Masuda, H.; Taga, T.; Osaki, K.; Sugimoto, H.; Yoshida, Z. I.; Ogoshi, H. *Inorg. Chem.* **1980**, *19*, 950-955.

(37) Although the differences between the parameters of five-coordinate [Fe(OEP)(2-MeHIm)]$^+$ and high-spin six-coordinate complexes are not rigorously statistically significant, it might have been expected that the five-coordinate complexes would have the longer bonds. The near equality serves to emphasize the fact that Fe–N_p bond distances in [Fe(OEP)(2-MeHIm)]$^+$ are significantly influenced by the overall charge on the complex.

(38) Weber, P. C.; Howard, A.; Xuong, N. H.; Salemme, F. R. *J. Mol. Biol.* **1981**, *153*, 399-424.

(39) Kobayashi, K.; Tamura, M.; Hayashi, K. *J. Biol. Chem.* **1980**, *255*, 2239-2242.

(40) Teraoka, J.; Kitagawa, T. *J. Biol. Chem.* **1981**, *256*, 3969-3977.

(41) Lanir, A.; Schejter, A. *Biochem. Biophys. Res. Commun.* **1975**, *62*, 199-203.

remains. Interestingly, the assignment of the spin state of the ferric forms of both proteins has proven to be difficult. Native forms of cytochromes *c'* have been assigned either high-spin or quantum-admixed intermediate spin states.[42,43] HRP appears to have complicated spin-state behavior that is related to its purity,[44] with both high- and quantum-admixed intermediate-spin states observed. Other investigators[45] have proposed chemical and thermal mixtures of high- and low-spin forms of ferric HRP. The structural data for $[Fe(OEP)(2\text{-MeHIm})]^+$ suggests a plausible explanation of such complicated spin-state behavior in these hemoproteins. For the $[Fe(OEP)(2\text{-MeHIm})]^+$ complex, the increased charge attraction of Fe(III) for the equatorial donor atoms leads to shortened Fe--N_p bonds; this is a likely feature of the hemoproteins as well. As we have noted elsewhere,[11] such a radical contraction of the core (relative to a normal high-spin species) should increase the tetragonal distortion and thereby decrease the energy differences between a pure high-spin state and an intermediate-spin state. It is thus credible that small, protein-induced perturbations could lead to differing magnetic properties in the coordination group $[Fe(Porph)(HIm)]^+$.

There is an interesting $\pi\cdots\pi$ interaction between pairs of $[Fe(OEP)(2\text{-MeHIm})]^+$ ions in both crystalline forms. The interaction in $[Fe(OEP)(2\text{-MeHIm})]ClO_4\cdot CH_2Br_2$ is shown in Figures 6 and 7. These two ions are related by an inversion center between them; consequently, the two porphinato cores are exactly parallel. Figure 7 is a view perpendicular to the porphinato planes that shows the "slipped" nature of the $\pi-\pi$ complex. Figure 6 the separation between the two porphinato planes which is a tight 3.312 Å. The Fe···Fe' distance is 4.280 Å, and the Ct···Ct' separation is 3.635 Å. The arrangement can be formally derived from two completely eclipsed porphinato cores which are then laterally shifted with respect to each other by 1.49 Å in the direction of an Fe–N_p bond. The arrangement in this $\pi-\pi$ complex is nearly identical with that observed in five-coordinate low-spin $[Fe(OEP)(NO)]ClO_4$[46] where the interplanar separation is 3.362 Å, the Ct···Ct' distance is 3.652 Å, and the lateral shift is 1.43 Å. The interaction between pairs of ions in $[Fe(OEP)(2\text{-MeHIm})]ClO_4\cdot CHCl_3$ is depicted in Figures 3S and 4S (supplementary material). The interaction between these ions is not quite as tight with Fe···Fe' = 4.60 Å, Ct···Ct' = 4.04 Å, and an interplanar spacing of 3.42 Å.

Dimeric porphyrin species have been previously characterized in solution by NMR[47] and EPR[48] techniques. The derived structures are similar to those observed for $[Fe(OEP)(2\text{-MeHIm})]ClO_4\cdot CH_2Br_2$ in the solid state, although the interplanar spacing and lateral shift are larger for the solution species. The appearance of $\pi-\pi$ dimers in both solid-state forms of $[Fe(OEP)(2\text{-MeHIm})]^+$ suggests a strong tendency to form dimers—which might persist to a significant extent in solution. Such dimer formation, even with modest thermodynamic stability, should have subtle but significant effects on the values of K_1 and especially K_2, the first and second ligand-binding constants. K_2 should decrease with increasing stability of the $\pi-\pi$ dimer since the dimer must be disrupted to coordinate the second axial ligand. We believe that such an effect contributes to the isolation of five-coordinate $[Fe(OEP)(2\text{-MeHIm})]^+$. However, this effect would not be applicable in tetraphenylporphyrin and related derivatives where the bulky phenyl groups would inhibit $\pi-\pi$ dimerization. Thus, an explanation of the noted[11] synthetic differences between OEP and TPP systems can be given. A decrease in K_2 in ferric octaethylporphyrinate and other alkyl-substituted porphyrin derivatives is not dependent on a hindered axial ligand; however, the importance of the effect in isolating five-coordinate species does depend on the relative magnitudes of K_1 and K_2. Another effect which could modulate magnitudes of K_1 and K_2, in favor of isolating five-coordinate species in the OEP system, is an electronic effect. K_2 is larger than K_1, at least in part, because of a spin-state change to low spin that occurs on forming six-coordinate species. However, cis effects on spin state[49] in iron(III) porphyrinates stabilize low-spin states more for TPP complexes than OEP complexes. This effect should increase K_2 more in the TPP derivatives than in the OEP species.

Yoshimura and Ozaki[5a] have measured stability constants for the binding of a series of hindered and unhindered imidazoles to protohemin chloride. They find that both K_1 and K_2 decrease for sterically hindered imidazoles relative to unhindered ligands but with K_2 decreasing more rapidly. Thus, for sterically hindered ligands, $K_2 \lesssim K_1$, but for unhindered ligands, $K_2 \gg K_1$. A limited amount of data for analogous Fe(TPP)Cl systems[5b] suggests that there are indeed differences in the binding constants that are consistent with the notion that $\pi-\pi$ complexes have an effect on K_2 in the protohemin systems but not the tetraphenylporphyrin systems. An adequate assessment of the importance of $\pi-\pi$ dimer formation on binding constants will require more directly comparable data than are currently available. Finally, it should be noted that another important factor in the isolation of monoimidazole species, difficult to assess in any quantitative fashion, is the solubility of the desired and undesired species under the crystallization conditions.[50]

Other than the $\pi-\pi$ dimer interactions described, there are no unusual packing interactions in the solid. The closest nonbonded contacts are between the perchlorate oxygen atoms and the porphyrin peripheral ethyl groups. Two contacts are ~3.1 Å; others ranged from 3.3 Å upward.

Summary. The preparation of a five-coordinate imidazole-ligated ferric porphyrinate has been conclusively demonstrated. A possible stabilizing factor in the synthesis is the close pairwise $\pi-\pi$ interaction between porphinato cores. The coordination group has shorter Fe–N_p bonds and smaller iron(III) atom displacements than those of the [Fe(Porph)X] class, the apparent consequence of the overall +1 charge of the complex. The complex, $[Fe(OEP)(2\text{-MeHIm})]^+$, displays magnetic moments consistent with an $S = {}^5/_2$ state and displaying weak antiferromagnetic coupling at low temperature. Detailed Mössbauer data are consistent with this picture.

Acknowledgment. We thank the National Institutes of Health for support of this work under Grants HL-15627 (WRS) and HL-16860 (GL) and the National Science Foundation under CHE80-26812 (CAR).

Supplementary Material Available: Figures 1S and 2S, computer drawn models of the two independent molecules, Figures 3S and 4S, diagrams of the $\pi-\pi$ interactions, Tables IS and IIS, atomic coordinates, isotropic temperature factors, and rigid group parameters, Table IIIS, anisotropic temperature factors, Tables IVS and VS, bond distances and angles, Table VIS, a listing of observed and calculated structure factors (×10) for $[Fe(OEP)(2\text{-MeHIm})]ClO_4\cdot CHCl_3$, Table VIIS, anisotropic temperature factors, Table VIIIS, fixed hydrogen atom parameters, and Table IXS, observed and calculated structure amplitudes (×10) for $[Fe(OEP)(2\text{-MeHIm})]ClO_4\cdot CH_2Br_2$ (59 pages). Ordering information is given on any current masthead page.

(42) Maltempo, M. M.; Moss, T. H.; Cusanovich, M. A. *Biochim. Biophys. Acta* **1974**, *342*, 290-305.
(43) Maltemp, M. M. *J. Chem. Phys.* **1974**, *61*, 2540-2547. Maltempo, M. M.; Moss, T. H. *Q. Rev. Biophys.* **1976**, *9*, 181-215.
(44) Maltempo, M. Mm.; Ohlsson, P.-I.; Paul, K.-G.; Petersson, L.; Ehrenberg, A. *Biochemistry* **1979**, *18*, 2935-2941.
(45) Tamura, M. *Biochim. Biophys. Acta* **1971**, *243*, 249-258.
(46) Scheidt, W. R.; Lee, Y. J.; Hatano, K. *J. Am. Chem. Soc.* **1984**, *106*, 3191-3198.
(47) Abraham, R. J.; Burbidge, P. A.; Jackson, A. H.; MacDonald, D. B. *J. Chem. Soc. B* **1966**, 620-626. Abraham, R. J.; Evans, B.; Smith, K. M. *Tetrahedron* **1978**, *34*, 1213-1219. Snyder, R. V.; LaMar, G. N. *J. Am. Chem. Soc.* **1977**, *99*, 7178-7184.
(48) Blumberg, W. E.; Peisach, J. *J. Biol. Chem.* **1965**, *240*, 870-876. Chikira, M.; Kon, H.; Hawley, R. A.; Smith, K. M. *J. Chem. Soc., Dalton Trans.* **1979**, 245-249. MacCragh, A.; Storm, C. B.; Koski, W. S. *J. Am. Chem. Soc.* **1965**, *87*, 1470-1476. Boas, J. F.; Pilbrow, J. R.; Smith, T. D. *J. Chem. Soc. A* **1969**, 721-723. Boyd, P. W. D.; Smith, T. D.; Price, J. H.; Pilbrow, J. R. *J. Chem. Phys.* **1972**, *56*, 1253-1263.
(49) Geiger, D. K.; Scheidt, W. R. *Inorg. Chem.* **1984**, *23*, 1970-1972.
(50) Work with an unhindered ligand (3-chloropyridine) has demonstrated that a five-coordinate substituted-pyridine complex can be prepared. However, it is found that the sample is always contaminated with the related bis-ligated species (Geiger, D. K.; Lee, Y. J.; Scheidt, W. R., work in progress).